JOURNAL OF GEOPHYSICAL RESEARCH, VOL. 93, NO. A8, PAGES 8613–8624, AUGUST 1, 1988

A Model of the Westward Traveling Surge and the Generation of Pi 2 Pulsations

P. L. ROTHWELL,[1] M. B. SILEVITCH,[2] L. P. BLOCK,[3] AND P. TANSKANEN[4]

A model of the westward traveling surge (WTS) and the generation of Pi 2 pulsations is presented here. Previous work concentrated on the motion of the WTS as a function of the precipitating electron energy and the concurrent generation of Pi 2 pulsations via a feedback instability. Now we look in more detail at the physical assumptions used in deriving the present model and the relations between the zero-order and the first-order solutions. Constraints are placed on the electron temperature asymmetry in the plasma sheet by requiring the Pi 2 pulsations to be bounded. It is found that the electron temperature anisotropy in the plasma sheet plays a major role in determining the direction in which the surge will propagate. Narrower surges require greater electron heating parallel to the magnetic field for poleward motion. More energetic electron precipitation is predicted to produce higher-frequency Pi 2 pulsations. Pulsations occur in multiple bursts with the time interval between bursts being shorter for shorter field lines. Initial amplitude and phase conditions are crucial in determining the pulse shape. The dominant period of the Pi 2 pulsation is found to be equal to twice the north-south dimension of the surge divided by a term which is proportional to the poleward velocity of the boundary. Finally, we show that the poleward surge velocities and Pi 2 pulsation periods as measured during the magnetospheric substorm of June 23, 1979, are consistent with our model. By noting the direction of the surge motion, one can use the model to estimate the magnitude of the polarization electric field. We find that it is consistent with zero for the onsets considered.

1. INTRODUCTION

The westward traveling surge (WTS) is a large region of auroral brightening that occurs near local midnight during substorm onsets. This region generally moves in a northwestward direction but at times is seen to move even eastward. The WTS has also been identified as the source of Pi 2 pulsations. What we have tried to do over the past few years is to develop a unified model for the WTS that explains both the motion of the surge and the generation of the Pi 2 pulsations [*Rothwell et al.*, 1984, 1986] (hereinafter referred to as paper 1 and paper 2, respectively). Our approach has been to model the ionospheric response to the precipitating electrons, rather than first identifying a promising magnetospheric mechanism and then determining its effect upon the ionosphere. While this may appear to be a somewhat backward approach, it has the advantage of starting with a tractable portion of the problem whose solution imposes conditions on the far less tractable magnetospheric source.

It is implicitly assumed in our model that the Inhester-Baumjohann current model [*Inhester et al.*, 1981; *Baumjohann*, 1983] represents the ionospheric currents inside the surge region (see Figure 1). It is the motion of this current system and its coupling to the magnetosphere that are the subject of this paper. While the recent Viking results indicate that the formation of a surge may be far more complex than previously thought [*Rostoker et al.*, 1987], the present model is still considered applicable for individual "hot spots" as well as for the more classical type of surge formation. Note, however, that our model deals with the ionospheric response to electron precipitation, so that direct changes in the magnetospheric source(s), such as the creation of a new hot spot or the fading of an old one, could produce dynamic effects not explainable by the present model.

The surge is created by an external electric field E_0 (Figure 1). This field drives a westward Pedersen current and a poleward Hall current. The Hall current is closed off into the magnetosphere by precipitating electrons along the poleward WTS boundary. The parameter α is a measure of current closure efficiency. *Lysak* [1986] has discussed the physical interpretation of the α parameter in terms of a possible magnetospheric source and its coupling to the flux tube ionosphere system. The reader is referred to that paper for more details. In our context, full closure ($\alpha = 1$) implies the full continuation of the ionospheric Hall current into the magnetosphere via field-aligned currents. In paper 1 we found that the WTS motion in the midnight sector is controlled by (1) the energy and flux of the precipitating electrons, (2) the electron-ion recombination rate, and (3) the degree of current closure on the poleward boundary of the surge.

On the basis of work by *Rostoker and Samson* [1981], *Samson* [1982], *Samson and Rostoker* [1983], *Pashin et al.* [1982], *Lester et al.* [1984], *Singer et al.* [1983, 1985], and *Gelpi et al.* [1987], there is clearly an observed relationship between the WTS and the generation of Pi 2 pulsations during substorm onsets. It is natural therefore to look for ways in which this relationship could occur using the current system shown in Figure 1. It was determined in paper 2 that perturbations in the north-south current in the WTS could produce standing waves due to the reflection from conductivity gradients along the surge boundaries. The surge serves as an ac port to an equivalent transmission line [*Sato*, 1982] formed by the attached magnetic field lines. Under the right conditions this port can resonate with the Alfvén waves that propagate along the equivalent transmission line, and Pi 2 pulsations will be generated from the ionosphere into the magnetosphere.

One basic idea in our model is that in addition to the ac (Alfvén wave) component, there is a quasi steady state (dc)

[1]Air Force Geophysics Laboratory, Hanscom Air Force Base, Massachusetts.
[2]Center for Electromagnetics Research, Northeastern University, Boston, Massachusetts.
[3]Department of Plasma Physics, Royal Institute of Technology, Stockholm, Sweden.
[4]Department of Physics, University of Oulu, Oulu, Finland.

Paper number 7A9356.
0148-0227/88/007A-9356$05.00

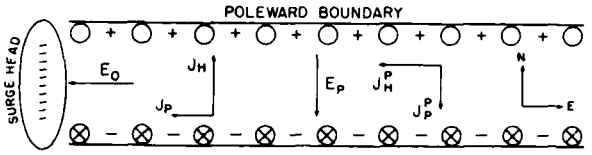

Fig. 1. Inhester-Baumjohann ionospheric current system [*Inhester et al.*, 1981; *Baumjohann*, 1983] for the westward traveling surge. This model forms the basis for the model presented in this paper.

component of electron precipitation that is dependent upon the temperature and density of the plasma sheet as well as on the potential difference along the field line. This dc component modulates the ionospheric conductivity and controls the speed and direction of the surge motion (paper 1).

The interior of the surge has a higher conductivity than the exterior because of enhanced precipitation. The current carried by precipitating energetic electrons in the interior surge region is assumed to be precisely balanced by upward flowing lower-energy ionospheric electrons. Therefore ionospheric current closure into the magnetosphere is assumed to occur only at the surge boundaries.

During substorm onsets there is a transient injection of electrons into the ionosphere from the plasma sheet. The associated transient current is assumed in our model to coincide with a transverse Alfvén wave [*Baumjohann and Glassmeier*, 1984] that initiates a feedback instability between the magnetosphere and the ionosphere in the surge region. This instability produces a complicated first-order ac component in the precipitation current that rides on top of the dc component as discussed above. The period of these oscillations tends to fall within the Pi 2 band (40–160 s). Now the first- and zero-order effects are not decoupled. The dc precipitation flux and energy control the frequency and damping rate of the Pi 2 pulsations, as we will see below. This approach is significantly different from that of *Lysak* [1986], which assumes that all the electron precipitation is associated with the Alfvén wave. Also, our model considers the ionospheric response to the Alfvén wave to be localized in the surge region, not global in nature, as in the work of *Zhu and Kan* [1987]. Comparisons of our work with that of *Kan et al.* [1984], *Kan and Kamide* [1985], and *Kan and Sun* [1985] are more fully discussed in section 6.

In the work of *Rothwell et al.* [1988] the results of *Fridman and Lemaire* [1980] were used to relate the dc precipitation flux and energy to the electron temperature anisotropy in the plasma sheet and to the potential drop along the field line. It was found that the damping rate of the Pi 2 pulsations as calculated from the results of Fridman and Lemaire closely followed the envelope of the growth curves as calculated from the feedback instability theory of *Sato* [1982]. The physical constraint that the Pi 2 pulsations be damped imposes a minimum allowable value on the ratio λ_x/α, where λ_x is the north-south dimension of the surge and α is the closure parameter, as defined above. It was found that narrower surge regions ($\sim$100 km) required preferential electron heating parallel to B (the magnetic field) in order for poleward motion to take place. For thicker surge regions ($\sim$300 km), poleward motion was allowed even when the electron temperature perpendicular to B dominated the parallel temperature. The precise value of the threshold ratio, which we denote by $(\lambda_x/\alpha)_t$, depends on the electron temperature ratio $T_\perp/T_\parallel$ in the plasma sheet. In this way the dynamics of the surge motion is controlled by the electron temperature anisotropy in the plasma sheet boundary.

In section 2 we will review the zero-order WTS theory as presented in paper 1. In section 3, Pi 2 pulsations will be treated according to the first-order theory developed in paper 2. Section 4 deals with the pulse shapes and their dependence on initial conditions and on the electron precipitation energy. Section 5 compares the model with three onsets observed on June 23, 1979. Finally, section 6 summarizes and presents the conclusions of the paper. In the appendix we have constructed a very simple convection model to justify the assumptions used in interpreting the experimental data.

2. Zero-Order Equations

In this section we briefly review the motion of the poleward boundary as derived in paper 1. Along the boundary is a conductivity gradient that must be consistent with the electron precipitation from the magnetosphere. The ionospheric ionization density in the gradient region is governed by the continuity equation as given by

$$\partial N/\partial t = Q j_\parallel e - \sigma_r N^2 \tag{1}$$

where Q is the energy-dependent ionization efficiency as given by *Rees* [1963], $j_\parallel e$ is the electron precipitation flux, σ_r is the electron-ion recombination rate, and N is the ionization density in the ionosphere. The current closure on the poleward boundary is given by

$$j_\parallel = -\alpha\, \partial J/\partial x \tag{2}$$

where J is the poleward Hall current and α is the closure parameter along the poleward boundary. We use a coordinate system in which x points north, y points west, and z points to the zenith. J is related to N by $J = \Sigma_H E_0$, where Σ_H is the height-integrated Hall conductivity. Now $\Sigma_H \simeq eN\,B$, where B is the magnetic field at the ionosphere.

By combining these relationships with (2), equation (1) becomes a wave equation if we momentarily ignore the recombination term. The phase velocity of this ionization wave is given by

$$V_x = QhV_d\alpha \tag{3a}$$

where h is the ionospheric height over which Q is significant and $V_d = E_0/B \simeq 0.25$ km s.

A solution for the velocity of the poleward boundary including electron-ion recombination effects has also been obtained in paper 1. Under the assumption of constant closure it was found that the equations greatly simplified by transforming the system to a coordinate frame moving at the boundary speed. (A more exact treatment of boundary propagation, however, must take into account time- and space-dependent closure.) In the moving frame the conductivity profile of the boundary remained constant and matched the Hall conductivity inside the surge at $x = 0$. (Note that x is the poleward coordinate here, rather than z, as in paper 1.) In the stationary frame the poleward boundary speed as given by equation (22) in paper 1 is

$$V = V_x - G\Sigma_{H0}{}^2 E_0 \alpha / j_{\parallel b} \qquad G = \sigma_r B/eh \tag{3b}$$

where $j_{\parallel b}$ is the upward closure current just where the boundary joins the surge interior and Σ_{H0} is the height-integrated Hall conductivity in the surge interior, which is maintained by a precipitating flux $j_{\parallel b}/e$. Using $\Sigma_{H0} = ehN_0/B$, where N_0 is the zero-order ionization level inside the surge region which is

given by $[Qj_{\|i}\, e\sigma_r]^{1/2}$, we have

$$V = V_x[1 - R_i/R_b] \tag{3c}$$

where $R_i = Q_i j_{\|i}\, e$ and $R_b = Q_b j_{\|b}\, e$ are the ionization rates in the surge interior and on the poleward boundary, respectively, and are approximately proportional to the energy flux. (Note that Q_i and Q_b are the respective ionization efficiencies, which are energy dependent [*Rees*, 1963].) If the ionization rate along the poleward surge boundary is greater than the ionization rate that is required to sustain the zero-order level of ionization (N_0) in the surge interior, then the surge moves poleward. If it is less, the surge moves equatorward, and the surge is stationary if the two ionization rates are equal. The model therefore predicts an auroral brightening along the poleward surge boundary that is coincident with the poleward leaps.

Note that in this treatment the conductivity profile has been assumed to remain stationary in the moving frame, which, in general, will not happen. A nonstationary conductivity profile leads to a time dependence in V which more accurately reflects the surge motion [*Sileritch et al.*, 1984]. The propagation speed of any profile, however, should increase in proportion to the excess of the ionization rate along the boundary over that of the surge interior. After all, that is what controls the propagation of the ionization wave. Therefore for short periods right after onset the measured velocities should be well represented by (3*a*) and (3*c*). This assumption is utilized below in comparing the model with data for the three substorm onsets of June 23, 1979, when data for the time evolution of the conductivity gradient are unavailable.

3. First-Order Equations

It is well documented that Pi 2 pulsations are fundamentally related to auroral breakup and substorm onsets [*Saito*, 1961; *Rostoker and Samson*, 1981; *Samson and Rostoker*, 1983; *Samson*, 1982]. As pointed out by *Samson* [1982], the Pi 2 pulsations occur simultaneously with or before all other ionospheric phenomena associated with breakup. These results are consistent with those of *Singer et al.* [1983, 1985] and *Gelpi et al.* [1987], who used magnetometer data from the Air Force Geophysics Laboratory (AFGL) magnetometer chain. Their results strongly imply that the Pi 2 source is located approximately 1 hour to the east of the western surge edge. *Pashin et al.* [1982] carried out a study on Pi 2 pulsations during the passage of the WTS under three successive auroral breakups. They found that the largest Pi 2 pulsation amplitudes were colocated in the region of the brightest auroras. In a similar study, *Baranskiy et al.* [1980] observed that the highest Pi 2 frequencies occurred near local midnight. *Stuart et al.* [1977] noted a correlation between the modulation in precipitating electron flux in the auroral zone and the coincident Pi 2 pulsations. *Maltsev et al.* [1974] suggested that Pi 2 pulsations were a result of the brightening of the aurora that led to an injection of an Alfvén wave from the ionosphere into the magnetosphere. This leads to field line oscillations and resonances in the Pi 2 frequency range.

On the basis of the large volume of evidence that Pi 2 pulsations and substorm onsets are related, it is therefore logical to explore whether the surge model developed in paper 1 can explain Pi 2 pulsations. We do this by looking at the first-order expansion of the basic equations. Equations (1) and (2) can be expanded into zero- and first-order terms. Along the boundary the zero-order terms reproduce the results in section 2, while they lead to a null result in the interior where N_0 is assumed constant. The first-order terms, on the other hand, are defined in the surge interior, where the analysis of *Sato* [1982] can be applied. They include the effect of Alfvén waves propagating along the attached field lines. Their effect at the ionosphere is seen as an equivalent ac impedance [*Sato*, 1982] which is given by

$$Z = iZ_0 \cot(\omega_r L/V_A - n\pi) \tag{4a}$$

where $Z_0 = \mu_0 V_A$ is the characteristic impedance of the equivalent transmission line, ω_r is the frequency of the Alfvén wave, n is the mode number, L is the length of the field line between the ionosphere and the equator, and V_A is the Alfvén speed ($\simeq 1000$ km/s) in the magnetosphere. Equation (4*a*) assumes perfect reflection of the Alfvén wave at the equator (i.e., zero magnetospheric conductivity), in contrast to the finite magnetospheric conductivity model developed by *Lysak* [1986]. The first-order precipitation current carried by the Alfvén wave is related to Z through $Z\hat{j}_{\|} = \nabla_\perp \cdot \hat{E}_\perp$. Implicit in this equation is the transmission line assumption and the propagation/reflection of Alfvén waves within the flux tube connecting the ionosphere to the magnetosphere. Now, as shown in paper 2, this relation when combined with the first-order expansion of (1) and (2) leads to dispersion relations for the frequency and growth rates of the individual modes.

We will briefly summarize the derivation as given in paper 2, with special care being taken regarding whether the quantities are defined on the surge boundary or in the surge interior. Following paper 2, the first-order continuity equation in the surge interior gives us

$$\partial N_i/\partial t = -Qhj_{\|i}\, eN_{0h} - 2\kappa N_i \tag{4b}$$

where

$$\kappa = \sigma_r N_{0h}/h$$

N_i is the height-integrated perturbed ionization density normalized to the height-integrated zero-order density, and $j_{\|i}$ is the perturbed (first-order) component of the field-aligned current, which is given by

$$j_{\|i} = -J_0 \nabla N_i/(1 - Z\Sigma_{H0}) \tag{4c}$$

where $J_0 = \alpha\Sigma_{H0}E_0$ is the net zero-order poleward current in the surge interior and is considered to be constant there. On the boundary, however, J_0 closes off into the magnetosphere, giving rise to the zero-order solutions derived above. Note that α is the closure parameter as defined on the surge boundary while Σ_{H0} is defined in the surge interior. The first-order current fluctuations give rise to no net current flow into and out of the interior region. Inserting (4*c*) into (4*b*) leads to defining the parameter $V_{xi} = \alpha Q_i h V_d$, which is analogous to the boundary velocity parameter as defined in (3*a*) and (3*c*) and which we now call V_{xb}. Note that $V_{xi} = V_{xb}$ only if the energy of the zero-order precipitation is the same in the surge interior as it is on the boundary. In the absence of measurements of the electron precipitation energy we assume that the velocity of the poleward boundary gives a reasonable measure of V_{xi}. This assumption is used below in section 5 and discussed in the appendix.

The first-order dispersion relations are then given by

$$\omega_r = 2\pi(V_{xi}/\lambda_x)/(1 + X^2) \tag{5}$$

$$\omega_i = \omega_r X - 2\sigma_r N_{0h}/h \tag{6}$$

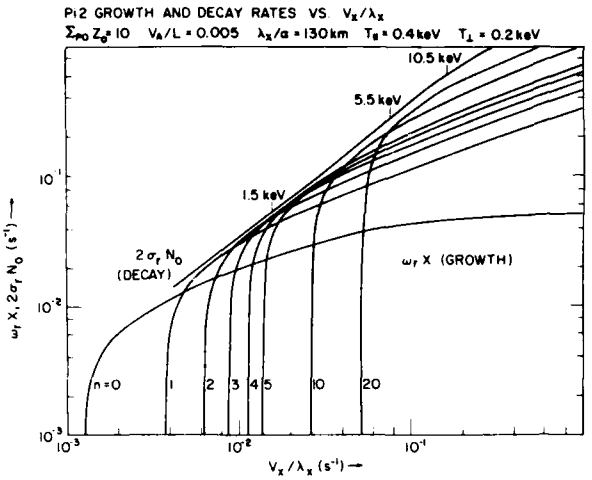

Fig. 2. Growth and damping curves for Pi 2 pulsations as derived from model. The growth curves are the nearly vertical lines, and the damping (decay) curve follows the envelope of the growth curves. The tick marks on the decay curve map the precipitating electron energies to the abscissa. The abscissa is plotted in units of V_x/λ_x, where λ_x is the north-south extent of the surge. In this example we took $\lambda_x \alpha = 130$ km, $V_A L = 0.005$, $\Sigma_{P0} Z_0 = 10$, $T_{||} = 0.4$ keV, and $T_\perp = 0.2$ keV. See text for definitions.

where ω_r and ω_i are the real and imaginary components of the frequency, respectively. X is equal to Z as defined in (4*a*) times the zero-order Pedersen conductivity in the ionosphere, Σ_{P0}. N_{0h} is the height-integrated equilibrium ionization density as expected from the zero-order (dc) electron precipitation inside the surge. From now on we set $N_{0h} = hN_0$, where N_0 is the local zero-order ionization density at the maximum ionization altitude for a given precipitation energy. (Note that in equation (18) of paper 2, h of equation (6) above is missing and the definition given in equation (11) of paper 2 should replace α in equations (12) and (16) of paper 2.)

Now if the zero-order electron precipitation energy inside the surge is of the order of a couple keV, then V_{xi} is approximately a couple kilometers per second (paper 1). In addition, if the north-south surge dimensions (λ_x) are of the order of hundreds of kilometers, then the characteristic frequency ($V_{xi}/2\lambda_x$) for ionospheric waves is close to that of Pi 2 pulsations. In order for a resonance to occur the characteristic ionospheric frequency just derived must be greater than or equal to the frequency of the fundamental toroidal mode for the attached field lines. *Singer et al.* [1981] found that the frequency of the fundamental toroidal mode was smallest at local midnight, reaching the Pi 2 range of 0.02 s^{-1} at $\Lambda = 66°$ and 0.005 s^{-1} at $\Lambda = 68°$. This suggests that the formation of a surge at auroral latitudes near local midnight sets up a resonance condition between the ionospheric waves and the magnetic field line oscillations which is triggered by the feedback instability, as described here.

There are both reactive ($+X$) and capacitive ($-X$) solutions to (5) and (6). The reactive solutions lead to growing Pi 2 pulsations from the feedback instability, while the capacitive solutions quench the instability. Reference is made to *Sato* [1982] and references therein regarding the details of these effects. *Samson* [1982] found that the Pi 2 oscillations originating from field-aligned currents are phase-shifted with respect to Pi 2 pulsations arising from the electrojet. In the present model this effect comes from the inductive nature of the field lines which allows growing solutions.

Note that the first-order dispersion relations also depend on the zero-order precipitation energy (i.e., the field-aligned potential drop) through V_{xi}. We use the theory of *Fridman and Lemaire* [1980] to estimate the magnitude of the zero-order precipitation for various field-aligned potential differences and plasma sheet parameters.

Figure 2 shows a separate plot of the Pi 2 growth and decay terms from (6) as a function of V_x/λ_x. The growth curves are the nearly vertical lines that tend to cross over each other. The damping curve is the nearly straight line that closely follows the envelope of the growth curves. The damping curve was calculated according to the *Fridman and Lemaire* [1980] theory with electron plasma sheet temperatures of $T_{||} = 0.4$ keV and $T_\perp = 0.2$ keV and with the density of the plasma sheet assumed to be 0.3 cm^{-3}. The tick marks denote the locations of various precipitation energies. Note that more energetic precipitation turns on higher-frequency modes. For Figure 2 we used $\Sigma_{P0} = 10$ mhos, $Z_0 = 1$ ohm, $V_A L = 0.005$ s^{-1}, and $\lambda_x \alpha = 130$ km.

If one inserts (5) into (6) and, for the moment, ignores the decay term, then one can find the maximum growth rate as a function of X. It is $\omega_r X = \omega_r = \pi V_x \lambda_x$ [*Rothwell et al.*, 1988] The condition that the Pi 2 pulsations be damped (i.e., that $2\sigma_r N_0 \geq \pi V_x \lambda_x$) leads to a minimum allowable threshold on $\lambda_x \alpha$, which to a high degree of accuracy is independent of the zero-order precipitation energy. This threshold depends on the plasma sheet parameters through the *Fridman and Lemaire* [1980] relation. We again set the plasma sheet number density to 0.3 cm^{-3} and calculated the threshold value of $\lambda_x \alpha$ by assuming a linear fit to the precipitation current for field-aligned potential drops between 5 kV and 50 kV. Figure 3 shows a plot of the threshold values $(\lambda_x \alpha)_t$ versus the electron temperature anisotropy $T_\perp/T_{||}$ in the plasma sheet. An analytical expression for the dependence of the threshold values on $T_\perp$, $T_{||}$, and the plasma sheet number density N_{ps} can be found. This is done by noting that $N_0 \simeq \Phi$, which leads to $(\lambda_x \alpha)_t \simeq T_\perp^{1.2} (T_{||}^{1.4} N_{ps}^{1.2})$, where Φ is the field-aligned potential drop.

There is a simple physical explanation for associating an enhanced $T_{||}$ with poleward motion of the conductivity slab. An increase in $T_{||}$ causes an increase in $j_{||h}$ [*Fridman and Lemaire*, 1980]. This increases the degree of modification of the conductivity gradient along the poleward boundary, which

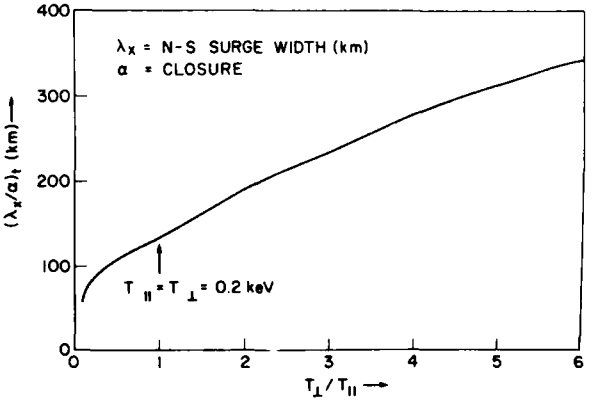

Fig. 3. The damping threshold for Pi 2 pulsations as a function of the electron temperature anisotropy in the plasma sheet using the model of *Fridman and Lemaire* [1980] for the precipitating electron flux. When the measured value of $\lambda_x \alpha$ exceeds the threshold value, the Pi 2 pulsations are damped.

causes a faster poleward surge expansion. The net effect is that anything that increases $j_{\|b}$ along the poleward boundary will cause a more northward motion of the surge region. An enhancement of $j_{\|b}$ also reduces the north-south polarization field (see Figure 1), which decreases the westward Hall current. Now an enhancement in temperature anisotropy (if it is global) will tend to impose an increase in $j_{\|}$ at the surge head. In our simplified steady state model this must be offset by a compensating decrease in the field-aligned potential [*Fridman and Lemaire*, 1980] at the surge head in order for $j_{\|}$ there to be continuous with the diminished westward ionospheric current. Our model therefore also suggests that enhanced $T_{\|}$ is accompanied by a brightening along the poleward boundary and a dimming in the region near the surge head.

The opposite argument holds for preferential electron heating perpendicular to the magnetic field in the plasma sheet. In that case the westward Hall current due to the polarization electric field is increased, and therefore the field-aligned potential at the surge head must increase to maintain current continuity [*Fridman and Lemaire*, 1980]. These effects favor a more westward motion of the surge region. The corresponding arguments suggest that enhanced $T_{\perp}$ will also cause a dimming along the poleward boundary accompanied by a brightening near the surge head.

In summary, according to our model, poleward surge motion is associated with electron heating in the plasma sheet parallel to the magnetic field. This heating could be caused by Fermi acceleration as the tail field becomes more dipolar. Preferential perpendicular heating from conservation of the first invariant is associated with westward surge motion.

What happens when the surge size is below the threshold limit with $\alpha = 1$? In that case we have positive growing pulsations. The period of the wave with the fastest growth rate, and therefore the period that is characteristic of the Pi 2 pulsation is $2\lambda_x / V_x$. In the limit of (3*a*) the surge is expanding at a velocity V_x, which means the surge triples in size in one pulsation period. The threshold for damping is quickly reached, and the pulsation has a finite amplitude. This feature validates the linear approximation used in deriving the Pi 2 pulsations. However, the rapid poleward motions mean that the zero-order parameter λ_x is changing on a time scale comparable with the first-order solutions. At the very least this leads to a time-dependent frequency which is outside the scope of our solutions. This problem is resolved if the surge moves in spurts or jumps. In that case the motion of the boundary induces a standing ionization wave inside the surge with a phase velocity which we assume to be close to the boundary velocity. From (5) this ionization wave is in resonance with the fastest growing Pi 2 mode ($X = 1$), and the present model applies between jumps. The assumption is that the jumps occur often enough that the critical surge size is reached in a timely manner and the pulsation amplitudes are not unreasonably large. A parallel resistance along the field line, such as that measured by *Weimer et al.* [1985, 1987], would also contribute to keeping the amplitudes finite (C. K. Goertz, private communication, 1987). During jumps a nonlinear treatment such as that of *Lysak* [1986, 1985], which incorporates the generation of PiB pulsations, is probably necessary. The observations of *Opgenoorth et al.* [1980] and *Bösinger et al.* [1981] suggest that PiB type pulsations lasted as long as the local onset-connected field-aligned currents were growing. On the other hand, if the multiplicative factor shown in (3*c*) is sufficiently small, then the change in frequency is adiabatic, and the present model applies in its entirety.

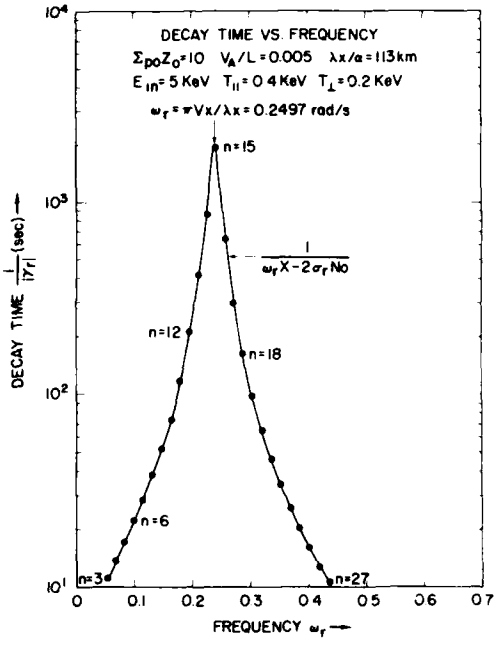

Fig. 4. Decay time of the individual modes shown in Figure 2 for a precipitating electron energy of 5 keV. The dots denote specific modes labeled *n*. Note that after several minutes the pulse will become quasi-monochromatic with the center frequency corresponding to the fastest growing mode. This is consistent with the data shown in Figure 9.

From Figure 3 we see that smaller damping threshold values for λ_x result when the plasma sheet electrons are preferentially heated parallel to the magnetic field. Now if the north-south surge dimension is below the threshold value for a given plasma sheet model, then α must be less than 1 in order for the Pi 2 pulsations to be damped. In paper 1 we showed that the direction of the surge motion is highly dependent on α. For α values less than 1, westward motion is predicted, while $\alpha \geqq 1$ allows poleward or even eastward motion. Therefore according to our model the electron temperature anisotropy in the plasma sheet together with the physical requirement that the Pi 2 waves be damped plays an important role in determining which way the current system of Figure 1 is going to move. The result is that embryonic surge regions require substantial preferential heating parallel to B for poleward leaps to occur. Some specific pulse shapes will now be examined.

4. Pi 2 Pulse Shapes

Recall from Figure 2 that the net decay rate of each mode is the difference between the decay curve ($2\sigma_r N_0$) and the individual growth curves at a specific precipitation energy. Figure 4 shows the calculated decay time for each mode for an incident energy of 5 keV and a surge size of 113 km. All other parameter values are as in Figure 2.

Thirty modes are excited in this particular example, and each mode is represented by a dot. Note that the decay time as a function of frequency is highly peaked at the frequency value found in section 3 for the maximum growth rate. What Figure 4 tells us is that the higher and lower frequencies quickly become damped and that the pulse propagates around a narrower frequency band at longer times. The period of this pulsation at the peak frequency is approximately 25 s, which is consistent with the Pi 2 frequency range.

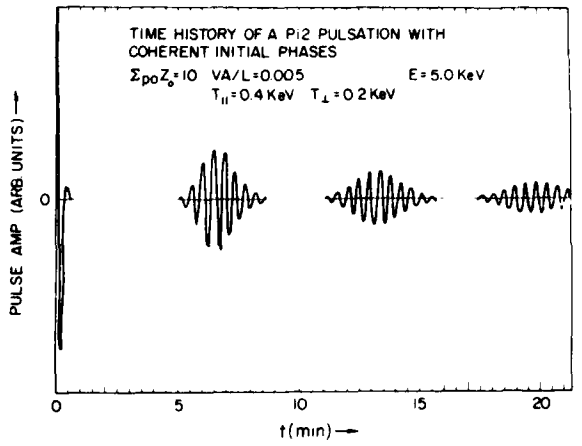

Fig. 5. A sample Pi 2 pulse shape (amplitude in arbitrary units) as a function of time for the same input parameters as shown in Figure 4. This is a linear superposition of all the modes assuming equal initial amplitudes and phases.

Figure 5 is a time history of this pulse. The initial conditions for this particular plot were chosen such that all modes were assumed to be excited with the same amplitude and at the same phase. The predicted time history as seen from Figure 5 is that of a large, initially overdamped pulse followed by series of "ringing" pulses of about 3 min in duration and 6–7 min apart. The time interval between "rings" becomes longer as the ratio V_A/L becomes smaller. Assuming V_A stays constant, this implies that period between rings is proportional to the length of the magnetic field line.

The specific shape of a given pulsation therefore depends very strongly on the initial conditions of its formation. The present model does not specify what these conditions are, but it does give the time evolution of the pulse once the initial conditions are given.

Despite this uncertainty, however, one can speculate on various possibilities. We redid the plot in Figure 5 using random initial phases (between 0° and 360°) for each of the 30 modes. Figure 6 shows the results. Note that the pulse has an extremely complicated shape during the first 5 min which completely masks the underlying sinusoidal dependence. In fact, one might interpret this section as a series of single pulses. The randomness, however, destroys the precise repeatability of the time profile, so that another example with the same parameter values would look somewhat different. It was found that even if the randomness in phase was as little as 20°, a difference with Figure 6 was not discernible. Given the complexity of the magnetosphere-ionosphere system and the irregularity of the driving precipitating flux, some incoherence in mode stimulation is to be expected. This incoherence destroys the precise cancellation between bursts, as seen in Figure 5, and the model simulates the actual data more closely.

Randomization of the initial amplitudes also destroys coherence and produces results similar to those seen in Figure 6 for random initial phases. Therefore Figure 6 is representative of a wide class of initial conditions. Now, regardless of the initial conditions, the selective filtering of the frequencies as seen in Figure 4 leads to a burstlike type of behavior after longer times. Therefore the precise nature of the initial conditions seems to dominate in only the first few minutes of the pulse train.

Figure 7 shows a coherent pulse train for an incident energy of 1.5 keV, $V_A/L = 0.001\ s^{-1}$, and $\lambda_x/\alpha = 125$ km. Note the same general features as in Figure 5: an initial overdamped pulse followed much later (30 min) by a finite pulse train. If this plot were of data, it would take a very astute observer to recognize that these two pulses are indeed one and the same. The pulsation burst evolves toward the mode with the longest decay time. (See the above discussion in regard to Figure 4.) The period of this mode is given by $T_p = 2\lambda_x/V_x$ and in this case is equal to 122 s, as opposed to 25 s for a 5-keV electron precipitation energy. Therefore one testable element of our model is that the frequency of the later, periodic portions of the Pi 2 pulsations should increase with the electron precipitation energy.

Figure 8 shows a pulsation with the same input values as in Figure 7 except that the initial phases are randomized as in Figure 6. Note that the horizontal scale is approximately one-half that of Figure 7. Randomization causes the various modes not to cancel and produces some interesting waveforms during the first few minutes. In fact, the first two peaks resemble a sequence of two overdamped single pulses, rather than a superposition of sinusoidal modes. The underlying sinusoidal structure does not become apparent until 10 min after onset. The pulsation shape is close to the measured Pi 2 waveforms shown in paper 2 and in Figure 3 in the work of *Southwood and Stuart* [1980].

It should be pointed out that the precise cancellation of the waveforms between bursts seen in Figures 5 and 7 implies a highly systematic structure for the nonlinear solutions which were obtained numerically. Investigation is proceeding as to what this structure is and whether it can be expressed in an analytical form or not.

We are also presently looking at the Fourier transform of these time profiles in order to make comparisons with data. Owing to the fact that the decay time is a function of frequency (see Figure 4), the frequency content of the wave is time dependent. This means that the Fourier transform is sensitive to the time at which the transform is taken. Nevertheless, our model predicts a spiky power density spectrum with the central spike located at the frequency corresponding to minimum damping.

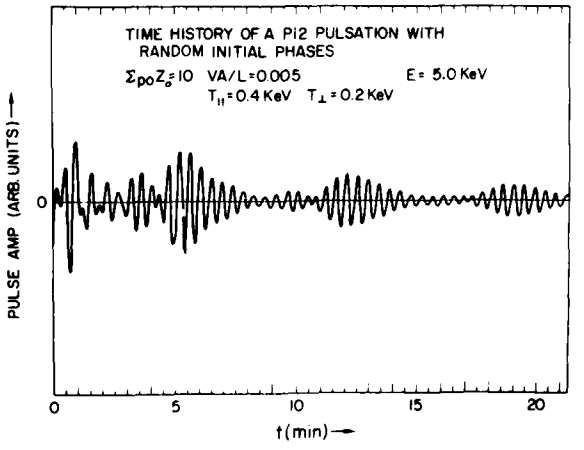

Fig. 6. The same as Figure 5 but now the linear superposition is carried out with random initial phases. Note the nonsinusoidal behavior at the beginning. This figure is more consistent with the data than Figure 5.

5. COMPARISON OF MODEL WITH EXPERIMENTAL DATA

A detailed study of three successive substorm onsets on June 23, 1979, was carried out using satellite-, balloon-, and ground-based particle and field data [*Tanskanen et al.*, 1987]. We now utilize these data to estimate the poleward velocity of the surge boundary and the north-south extension of the surge for each of the three onsets. These results are then used to estimate the period of the fastest growing mode, as described above. This period is then compared with the measured period of Pi 2 pulsations as seen by ground-based magnetometer stations.

For the following comparison we use Table 3 of *Tanskanen et al.* [1987]. The first onset was observed at Sodankylä (latitude 67.4°, longitude 26.6°, $L = 5.1$) at 2101 UT. Thirty seconds later, it was observed at Ivalo (latitude 68.6°, longitude 27.4°, $L = 5.7$), and 30 s beyond that, at 2102 UT, it was observed at Kevo (latitude 69.8°, longitude 27.0°, $L = 6.2$). Now Sodankylä, Ivalo, and Kevo are close together on the same meridian, so that the successive detection of the onset gives a good measure of the initial poleward surge velocity V. We find $V = 4.4$ km/s for the first onset. The westward component of the surge velocity V_w is found by noting that the onset occurs at the balloon SO622 (latitude 67.6°, longitude 5.1°, $L \simeq 6$) 10 min after it reached Sodankylä, which is along the same geographic latitude. Therefore $V_w = 1.6$ km/s for the first onset. The surge is estimated to include Sodankylä and Kevo, which gives a north-south extension λ_x of about 280 km. For a complete analysis it is necessary to know the energy and flux of the electron precipitation both inside the surge and along the poleward boundary. Unfortunately, this level of detail is not available. However, we do have riometer data which give an indication of the relative intensity of the precipitation energy. The precipitation was most intense during the first onset. Therefore for this period we make the assumption that the ionization rate along the surge boundary exceeds the ionization rate inside the surge and that $V = V_{xh} = V_{xi} = 4.4$ km/s. (See (3*c*), the discussion following (4*c*), and the appendix for more details regarding these assumptions.) In this case the period ($T_p = 2\lambda_x / V_{xi}$) of the fastest growing mode is 127 s. Now the magnetometer results are Fourier-analyzed and plotted in frequency versus time contour plots, where each contour represents a constant amplitude. The contour plot of Kevo is shown in Figure 9, with the onsets denoted by short vertical lines. Just after the first two onsets the maximum amplitude (the dense band of concentric ellipses) occurred at approximately 120 ± 10 s, with a secondary peak at ~95 s. A plot of the Ivalo magnetometer data shows similar results although at lower amplitudes. The delay of the monochromaticity relative to the substorm onsets is consistent with the model results shown in Figures 6 and 8. For the first onset the delay is approximately 6–8 min. Considering the assumptions involved in calculating V_{xi} and λ_x, the excellent agreement (127 s versus 120 ± 10 s) may be somewhat fortuitous. However, the overall agreement between the experimental observations and the model lends a great deal of credence to the model's basic veracity.

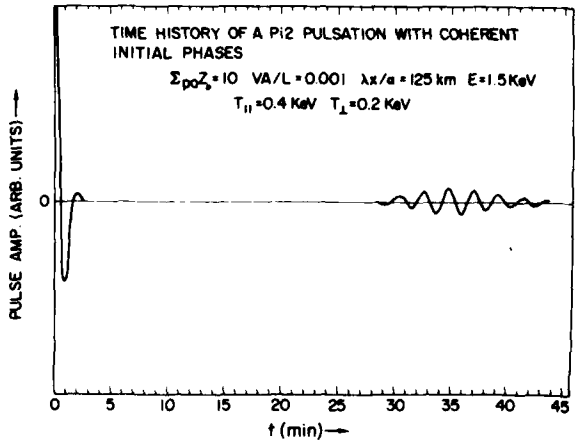

Fig. 7. Time history of a Pi 2 pulsation with coherent initial phases and 1.5 keV incident energy. Note the longer period in comparison with Figure 5. The higher the incident energy the higher the frequency of the expected pulsations.

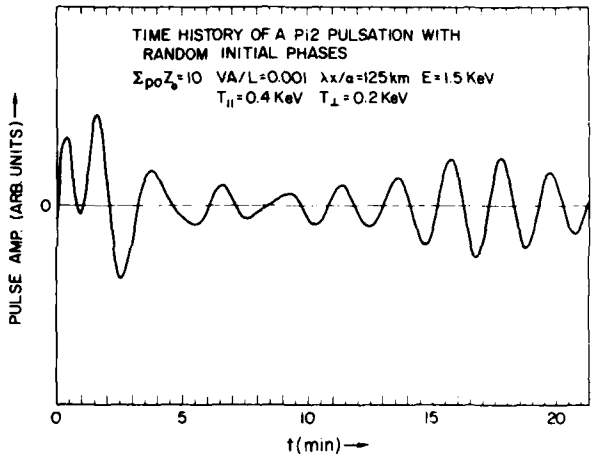

Fig. 8. Time history of a Pi 2 pulsation with random initial phases and 1.5 keV incident energy. This pulse profile is very similar to profiles observed in the data (see, for example, *Rothwell et al.* [1986]). Note once again that the pulsation becomes almost monochromatic after about 10 min.

The second onset of Sodankylä (2107:30 UT) gives similar results. The poleward velocity between Sodankylä and Ivalo (2109 UT) is 1.5 km/s, and between Ivalo and Kevo (2109:30 UT) it is 4.4 km/s. The lower velocity between Sodankylä and Ivalo is explainable by the fact that the riometer absorption at Sodankylä has dropped to 0.7 dB from 1.3 dB as in the first onset. This implies less intense precipitation and hence a slower speed according to our model. The westward velocity component is found as before and is 1.8 km/s. We take the north-south surge dimensions to be between Sodankylä and Kevo as before, which gives 286 km in geographic coordinates. Now Andenes is geographically south but magnetically north of Kevo [see *Tanskanen et al.*, 1987, Table 3]. If one prefers the surge dimensions in magnetic coordinates, then the surge should be measured between Andenes and Sodankylä. In that case we find a distance of 289 km. The period of the fastest growing mode is therefore predicted to be 131 s. Now from Figure 9 we see that the period with the maximum amplitude is around 127 s, which occurs approximately 10 min after the second onset. The agreement is again excellent.

The third onset is more complicated for two reasons. The first reason is that the poleward boundary now passes by the stations KA 0622 (latitude 70.4°, longitude −7.2°, $L \simeq 8.5$) at 2140 UT, Björnöya (latitude 74.5°, longitude 19°, $L = 9.4$) at 2143 UT, and HO 0623 (latitude 72.9°, longitude 7.6°, $L \simeq 9.2$)

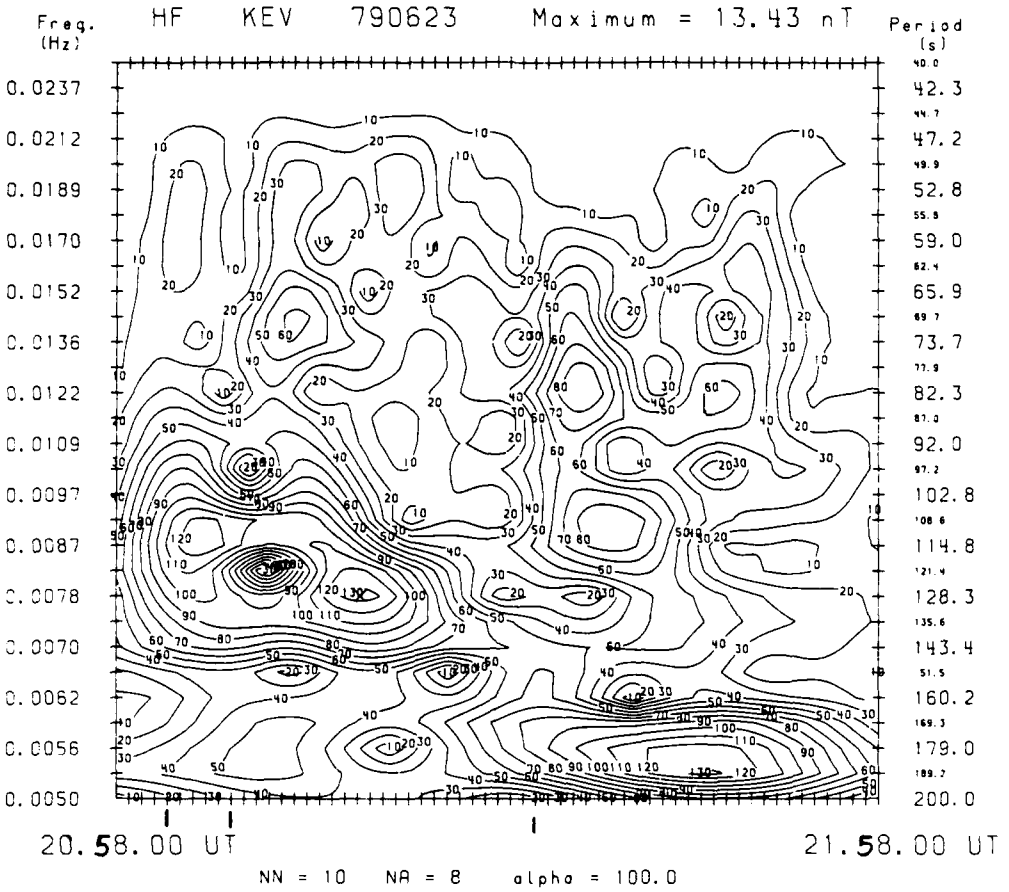

Fig. 9. A contour plot of the filtered magnetometer data taken at Kevo during the period of three substorm onsets on June 23, 1979. Each contour represents a given amplitude which is plotted as a function of frequency. The abscissa is universal time in units of minutes starting at 2058:00 UT and ending at 2158:00 UT. The three heavy tick marks show the time of the three onsets. The more concentrated areas of concentric rings denote regions of more intense wave energy. It is shown in the text that these regions are numerically very consistent with the expected Pi 2 periods as derived from our model. Also, the lengthening of the Pi 2 period with successive onsets is consistent with the poleward expansion of the surge as predicted by the model.

at 2145 UT. These stations are separated in both latitude and longitude, which complicates the determination of the velocity components. The second reason is that the third onset is much less intense than the previous two onsets according to the riometer data. This implies from our model (see (3c)) that the measured poleward velocity could be much less than the V_{xi} parameter needed to estimate the associated Pi 2 period. We find that the measured poleward velocity is approximately equal to 0.25 km/s and the westward velocity is 2 3 km/s, where the spread is due to whether one works in geographic or magnetic coordinates. We therefore assume for the third onset that the precipitation energy is the same inside the surge as on the poleward boundary and as during the previous two onsets. According to this scenario the surge moves because of an enhancement of the boundary precipitation flux of a few percent over the precipitation flux inside the surge. The old value of 4.4 km/s for V_{xi} will therefore be used.

The north-south extent of the surge during the third onset is also difficult to quantify because of the spatial separation of the stations. On the basis of Figure 3 of *Tanskanen et al.* [1987] we estimate the surge to be between Ivalo ($L = 5.7$) and Björnöya ($L = 9.4$), which gives a distance of 689 km. This implies a Pi 2 period of 312 s, which is still comparable to the measured value of roughly 190 $\pm$ 30 s seen 12 min after onset in Figure 9. The important thing to note from Figure 9 is the definite lengthening of the Pi 2 period as the surge expands poleward. This effect is predicted by the present model, as the period of the fastest growing mode is proportional to λ_x.

The model can be used to extract other important information about the onsets using this important data set. From the value of V_{xb} of 4.4 km s and noting that the measured value of E_0 was approximately 20 mV m during the first two onsets, we use (3a) to estimate the precipitating electron energy that is responsible for the surge movement as being 1.7 keV. (Note that $QH = 5\varepsilon^{1.2}$ ions per incident electron (see paper 1), where ε is the precipitating energy.) Using the direction of the surge motion, one can also estimate the magnitude of the north-south polarization electric field inside the surge. (The measured value of the north-south electric field component is 25 mV m, which includes the convection electric field which may dominate.) Equation (12) of paper 1 can be rewritten as

$$\tan \gamma_s = (R - E_p/E_0)/(1 + RE_p/E_0) \qquad (7)$$

where γ_s is the angle of the surge motion relative to west, R is the ratio of the height-integrated Hall to Pedersen conductivities, and E_p (which is positive, pointing south) is the polarization electric field. (The relation $E_p = E_0 R(1 - \alpha)$ has been used in deriving (7).) Equation (7) can be reexpressed as

$$E_p E_0 = (R - \tan \gamma_s)(1 + R \tan \gamma_s) \quad (8)$$

Grafe [1982] has noted that R ordinarily ranges between 1 and 4, with some rare cases in which R is greater than 4. It is also noted that R tends to decrease with enhanced substorm activity and widening of the electrojet. Using (8), it is found that for the first onset, -2.2 mV m ($R = 1$) $< E_p < +2.1$ mV m ($R = 4$), which is consistent with full closure of the poleward Hall current into the magnetosphere. (A value of 2.75 was used for $\tan \gamma_s$.) The second onset is like the first, and the third is too complex to be treated here.

We conclude therefore that the three onsets discussed are consistent with our model. Not only is there quantitative agreement with the predicted Pi 2 periods, but the observed time delay for the Pi 2 pulsations to approach a monochromatic signal is compatible with a frequency-dependent decay time, as derived above. In particular, the predicted scaling of the Pi 2 periods with the surge size and poleward velocities seems convincing. The model may also be useful as a tool in separating out the polarization and convection electric fields.

6. Discussion

We have presented a unified model for the motion of the westward traveling surge and the generation of Pi 2 pulsations during substorm onsets. Using the Inhester-Baumjohann ionospheric current system shown in Figure 1, it was shown that the zero-order electron precipitation current (dc) controlled the surge motion. The dynamics of the surge boundary was found for a constant conductivity profile, which led to a constant value of the boundary propagation speed V. This value is assumed to give a reasonable estimate of the initial surge velocity, which in a more realistic treatment must be time dependent, as the conductivity profile evolves in time. The first-order equations led to dispersion equations in the Pi 2 frequency range. The present Pi 2 model was determined to be valid between surge jumps when the surge was considered quasi-stationary or when the surge moved sufficiently slowly. During jumps it is suggested that a nonlinear theory such as that of *Lysak* [1986] is more realistic, since it predicts the presence of PiB pulsations, which have been observed by *Opgenoorth et al.* [1980] and *Bösinger et al.* [1981].

The present model leads in a natural way to using the results of *Fridman and Lemaire* [1980] and *Fälthammar* [1978] in determining the dc precipitation current, which plays a major role in damping the Pi 2 pulsations. The physical requirement that the Pi 2 pulsation be dampled puts a lower bound on the ratio of the north-south surge dimension and the closure parameter α. This bound depends on the electron temperature anisotropy in the plasma sheet and plays a crucial role in determining the direction of surge motion. Growing models were found to be quenched by the poleward expansion of the surge.

Now because of the dispersive nature of the Pi 2 pulsation, its frequency composition changes with time. The time profile of the pulsation also is very sensitive to the initial conditions. If all the modes are excited at exactly the same time (i.e., the same phase), then the time profile is that of a highly damped wave followed by periodic sinusoidal bursts. Even a small admixture of phases at $t = 0$, however, will cause the pulse to exhibit nonsinusoidal behavior just after onset which evolves into sinusoidal behavior several minutes later. This effect appears to be real, as seen from Figure 9 and from examples of the AFGL magnetometer data (paper 2).

Three onsets that were observed on June 23, 1979, were compared with the model. It was found that the poleward surge velocities and the estimated north-south surge dimensions led to predicted Pi 2 pulsation periods that were consistent with the measured values. The period of the observed Pi 2 pulsations became longer as the surge expanded, which is consistent with the model. It was also shown how the model might be used as a tool in determining the polarization electric field in the presence of a strong convection electric field.

Let us now consider a scenario for auroral breakup based on the present model. Initially, an incipient surge region of a few tens of kilometers forms near local midnight [*Akasofu*, 1974]. It consists of an enhanced ionization region in the ionosphere that contains the current system shown in Figure 1. Now if the ionization rate at the surge's poleward boundary is equal to the ionization rate in the surge interior, the surge is stationary [*Rothwell et al.*, 1988]. If the rate at the boundary is greater, then the surge moves poleward.

It is interesting to compare the present model with the experimental observations of substorm breakup described by *Akasofu* [1974, p. 647].

> The first indication of a substorm is a sudden brightening of one of the quiet arcs (discrete auroras) lying in the midnight sector or the sudden formation of an arc in that region. A typical substorm develops when this arc is located near the equatorward boundary of the belt of discrete auroras, but near the poleward boundary of the belt of diffuse auroras. In most cases, the brightening of an arc or the formation of an arc is followed by its rapid poleward motion, resulting in an 'auroral bulge' around the midnight sector. The so-called 'break-up' occurs in the bulge: a quiet curtain-like form appears to be disrupted and scattered over the sky.

In terms of our model and Akasofu's observations, auroral breakup occurs when an Inhester-Baumjohann type ionospheric current system forms near the poleward boundary of the diffuse aurora. The poleward Hall current in this embryonic system is closed off into the magnetosphere through the formation of the arc described by Akasofu.

If a field-aligned potential drop should switch on over the poleward boundary, the arc there would brighten and move poleward with a speed proportional to the magnitude of the potential drop (see papers 1 and 2 and *Rothwell et al.* [1988]). The boundary motion excites standing ionospheric waves in the surge interior which have phase velocities which are determined by the initial boundary speed. Because of their long wavelengths (~ 100 km) these ionospheric waves could be difficult to detect owing to the turbulent nature of the ionosphere over much smaller distances. If the associated frequencies of the ionospheric waves are greater than or equal to the frequency of the fundamental toroidal mode of the attached field line [*Singer et al.*, 1981], then a resonance can occur through the feedback instability.

The resonance is considered to be damped by electron-ion recombination in the ionosphere. Now the precipitating flux, which causes the damping, is a function of the electron temperature asymmetry in the plasma sheet [*Fridman and Lemaire*, 1980]. If this flux is insufficient to fully close off the

poleward Hall current in the ionosphere, then the α parameter is less than 1. This means that the surge will move predominantly westward (paper 1) and the coincident Pi 2 pulsations will be strongly damped. (For a given surge size, if α is less than 1, it is more probable that the threshold criterion for damping is met.) A value of α less than 1 implies weaker precipitation, which for a given field-aligned potential drop implies enhanced perpendicular electron heating in the plasma sheet according to the model of *Fridman and Lemaire* [1980]. Perpendicular electron heating in the plasma sheet would therefore cause predominantly westward surge motion and strongly dampled Pi 2 pulsations. On the other hand, parallel electron heating in the plasma sheet (α greater than or equal to 1) would cause predominantly poleward motion and, possibly, the momentary presence of growing Pi 2 pulsations. As mentioned above, the poleward expansion of the surge limits the amplitude of the pulsations when the damping threshold is reached.

Therefore according to the present model the substorm is associated with enhanced precipitation, poleward surge motion, and the generation of finite amplitude Pi 2 pulsations. All these effects are common features associated with substorms and, as shown, may be caused by preferential electron heating in the plasma sheet parallel to the magnetic field.

While the present model appears to be very successful in explaining a variety of observations during substorm onsets, it is by no means all-inclusive. It is still a linear approximation to a highly nonlinear problem where the nonlinear effects apparently are strongly damped over relatively short time scales. We have not addressed, for example, how the initial Alfvén wave transmits the information about the short circuiting of the tail current between the magnetosphere and the ionosphere during the creation of the substorm current wedge [*Baumjohann and Glassmeier*, 1984], nor have we touched upon the possibility of the Alfvén waves creating a field-aligned potential drop through turbulence [*Lysak and Dum*, 1983; *Lysak*, 1985]. Moreover, a more realistic treatment of Alfvén wave propagation in the magnetosphere and ohmic losses in the ionosphere [*Goertz and Boswell*, 1979] is needed. Finally, there may be more than one source of Pi 2 pulsations. *Edwin et al.* [1986], for example, suggest that Pi 2 pulsations arise from an impulsive source of MHD wave energy in the plasma sheet. The fast magnetoacoustic waves that are produced propagate dispersively through the plasma sheet, which gives rise to finite Pi 2 type wave packets nearer the Earth.

It is clear that an important future consideration would involve placing the mechanisms developed here into a more global framework. In this regard it should be mentioned that *Zhu and Kan* [1987] have combined the temporal propagation mechanisms of paper 1 with the global assumption of the closure parameter developed by *Kan et al.* [1984] and *Kan and Kamide* [1985]. Moreover, *Kan and Sun* [1985] have described a global model for simulating the westward surge and Pi 2 pulsations. In this model they combine steady state assumptions inherent in the work of *Kan and Kamide* [1985] with a description of Alfvén waves bouncing between a magnetospheric source and the ionosphere. Their procedure results in a temporal scheme involving the discrete bouncing of the Alfvén waves into the ionosphere and the generation of "steplike" Pi 2 waveforms. Note that in both works the ionosphere plays an active role and is a source of Pi 2 pulsations. In the present work a feedback instability is the driving mechanism, while in the work of *Kan and Sun* [1985] a feedback instability was not included. Multipoint measurements are necessary in order to determine which of these models are correct under different substorm conditions.

APPENDIX

Comparison of our model predictions for Pi 2 periods with data requires knowledge of the precipitation energy and flux both on the poleward boundary and in the surge interior. This would allow a direct calculation of V_{xi}. Since this information was not available, it was necessary to assume that the measured velocity V of the poleward boundary was equal to V_{xi}. Now (3*c*) implies that $V = V_{xi}$ only when the ionization rate along the poleward boundary is much greater than the ionization rate in the surge interior. From (3*a*) we see that $V_{xi} = V_{xb}$ only if the electron precipitation energy in the surge interior is equal to the precipitation energy on the surge boundary. We assume that this latter condition is satisfied during the onsets considered and develop a model to ascertain the validity of assuming $R_i \ll R_b$. Now enhanced precipitation on the poleward boundary implies a depletion of the plasma associated with attached flux tubes [*Atkinson*, 1984]. Therefore as the plasma convects earthward through the surge interior, it is a weaker source of precipitation than it is on the boundary, and $V \simeq V_{xi}$ from (3*c*).

We now make a very simple model that illustrates the physical concepts involved. It will be shown that for reasonable substorm values of precipitation current (~ 10 μA m^{-2}) along the poleward boundary the precipitation flux in the surge interior will be sufficiently small that $V \simeq V_{xi}$ from (3*c*). This will validate our assumptions. Consider the equatorial plane and a plasma with a number density $N_{ps} = 0.3$ cm^{-3} convecting toward the Earth at a speed $V_c \simeq 50$ km/s [*Huang and Frank*, 1986]. This plasma is estimated to contribute to the electron precipitation flux over a field line length of approximately $LR_E 3$, where L is the L shell on which the precipitation takes place and $R_E = 6.37 \times 10^6$ m. Therefore the total particle flux which is available for precipitation is $N_{ps}V_c LR_E\lambda_{ye} 3$, where λ_{ye} is the east-west extent of the surge region as seen in the equatorial plane. This flux is assumed to be totally depleted by precipitation along the surge's poleward boundary and in the surge interior. The total electron flux precipitated along the boundary is given by $j_{\|be}\lambda_{be}\lambda_{ye}\, e$ and in the interior by $j_{\|ie}\lambda_{xe}\lambda_{ye}\, e$. Here λ_{be} is the extent of the conductivity gradient along the poleward surge boundary (as seen at the equator), and λ_{xe} is the north-south extent of surge (also as seen at the equator). Now particle flux conservation along the field line implies $j_{\|be}\lambda_{be}\lambda_{ye} = j_{\|b}\lambda_b\lambda_y$ and $j_{\|ie}\lambda_{xe}\lambda_{ye} = j_{\|i}\lambda_x\lambda_y$, where the quantities without the subscript e are defined at the ionosphere.

By equating the total inward convecting flux to the flux at the poleward boundary plus that in the surge interior and using flux conservation along the magnetic field lines we finally have an expression for $j_{\|b}$:

$$j_{\|b} = \frac{eN_{ps}V_c R_E L^{5/2}}{3\lambda_b\{(j_{\|i}/j_{\|b})(\lambda_x/\lambda_b) + 1\}} \quad \text{A/m}^2 \qquad \text{(A1)}$$

where the azimuthal scaling factor for a dipole field ($\lambda_{ye}/\lambda_y = L^{3/2}$ [*Lotko et al.*, 1987]) has been used. Now if we make the reasonable assumption that $\lambda_b = 20$ km and that $L = 6$ and $\lambda_x = 280$ km, which corresponds to the first two onsets of June 23, 1979, then (A1) can be rewritten using the numerical values

given above as

$$j_{\|b} = 22.5\{14 j_{\|i}/j_{\|b} + 1\} \quad \mu A/m^2 \qquad (A2)$$

Now from (3*c*) the surge is stationary if the current ratio is equal to 1. This corresponds to a boundary precipitation current density of 1.5 μA m^2. For $V \simeq V_{xi}$ the current ratio must be approximately 0.1 or less. This implies from (A2) that $j_{\|b}$ should lie between 9.4 and 22.5 μA/m^2, which is easily realized. We therefore conclude, on the basis of this very simple convection model, that the assumptions used to analyze the Scandinavian data were reasonable and appropriate.

Acknowledgments. It is with pleasure that we acknowledge the helpful comments of Carl-Gunne Fälthammar from The Royal Institute of Technology in Stockholm, Sweden, and Nelson Maynard, William Burke, Howard Singer, and Michael Heinemann from the Air Force Geophysics Laboratory. One of the authors (M.B.S.) would like to acknowledge the support of U.S. Air Force contract F19628-85-K-0053. The clerical assistance of Linda Silva, Anne Rothwell, and Kathleen Sullivan is also appreciated.

The Editor thanks K.-H. Glassmeier and another referee for their assitance in evaluating this paper.

REFERENCES

Akasofu, S.-I., A study of auroral displays photographed from the DMSP-2 satellite and from the Alaska meridian chain of stations, *Space Sci. Rev.*, *16*, 617–725, 1974.

Atkinson, G., Field-aligned currents as a diagnostic tool: Result, a renovated model of the magnetosphere, *J. Geophys. Res.*, *89*, 217–226, 1984.

Baransky, L. N., V. A. Troitskaya, I. V. Sterlikova, M. B. Gokhberg, N. A. Ivanov, I. P. Khartchenko, J. W. Münch, and K. Wilhelm, The analysis of simultaneous observations of nighttime Pi 2 pulsations on an east-west profile, *J. Geophys.*, *48*, 1–6, 1980.

Baumjohann, W., Ionospheric and field-aligned current systems in the auroral zone: A concise review, *Adv. Space Res.*, *2*, 55–62, 1983.

Baumjohann, W., and K.-H. Glassmeier, The transient response mechanism and Pi 2 pulsations at substorm onset - Review and outlook, *Planet. Space Sci.*, *32*, 1361–1370, 1984.

Bösinger, T., K. Alanko, J. Kangas, H. Opgenoorth, and W. Baumjohann, Correlations between PiB type magnetic micropulsations, auroras and equivalent current structures during two isolated substorms, *J. Atmos. Terr. Phys.*, *43*, 933–945, 1981.

Edwin, P. M., B. Roberts, and W. J. Hughes, Dispersive ducting of MHD waves in the plasma sheet: A source of Pi 2 wave bursts, *Geophys. Res. Lett.*, *13*, 373–376, 1986.

Fälthammar, C.-G., Problems related to macroscopic electric fields in the magnetosphere, *Astrophys. Space Sci.*, *55*, 179–201, 1978.

Fridman, M., and J. Lemaire, Relationships between auroral electron fluxes and field-aligned potential differences, *J. Geophys. Res.*, *85*, 664–670, 1980.

Gelpi, C., H. J. Singer, and W. J. Hughes, A comparison of magnetic signatures and DMSP auroral images at substorm onset: Three case studies, *J. Geophys. Res.*, *92*, 2447–2460, 1987.

Goertz, C. K., and R. W. Boswell, Magnetosphere-ionosphere coupling, *J. Geophys. Res.*, *84*, 7239–7246, 1979.

Grafe, A., Estimated conductivity ratio Σ_H/Σ_P in the auroral electrojets in connection with the electrojet width and field-aligned currents, *Planet. Space Sci.*, *30*, 525–536, 1982.

Huang, C. Y., and L. A. Frank, A statistical study of the central plasma sheet: Implications for substorm models, *Geophys. Res. Lett.*, *13*, 652–655, 1986.

Inhester, B. W., W. Baumjohann, R. W. Greenwald, and E. Nielsen, Joint two-dimensional observations of ground magnetic and ionospheric electric fields associated with auroral zone currents, 3, Auroral zone currents during the passage of a westward traveling surge, *J. Geophys.*, *49*, 155–162, 1981.

Kan, J. R., and Y. Kamide, Electrodynamics of the westward traveling surge, *J. Geophys. Res.*, *90*, 7615–7619, 1985.

Kan, J. R., and W. Sun, Simulation of the westward traveling surge and Pi 2 pulsations during substorms, *J. Geophys. Res.*, *90*, 10,911–10,922, 1985.

Kan, J. R., R. L. Williams, and S.-I. Akasofu, A mechanism for the westward traveling surge during substorms, *J. Geophys. Res.*, *89*, 2211–2216, 1984.

Lester, M., W. J. Hughes, and H. J. Singer, Longitudinal structure in Pi 2 pulsations and the substorm current wedge, *J. Geophys. Res.*, *89*, 5489–5494, 1984.

Lotko, W., B. U. Ö. Sonnerup, R. L. Lysak, Nonsteady boundary layer flow including ionospheric drag and parallel electric fields, *J. Geophys. Res.*, *92*, 8635–8648, 1987.

Lysak, R. L., Auroral electrodynamics with current and voltage generators, *J. Geophys. Res.*, *90*, 4178–4190, 1985.

Lysak, R. L., Coupling of the dynamic ionosphere to auroral flux tubes, *J. Geophys. Res.*, *91*, 7047–7056, 1986.

Lysak, R. L., and C. T. Dum, Dynamics of magnetosphere-ionosphere coupling including turbulent transport, *J. Geophys. Res.*, *88*, 365–380, 1983.

Maltsev, Yu. P., S. V. Leontyev, and W. B. Lyatsky, Pi 2 pulsations as a result of an Alfvén impulse originating in the ionosphere during the brightening of aurora, *Planet. Space Sci.*, *22*, 1519–1533, 1974.

Opgenoorth, H. J., R. J. Pellinen, H. Maurer, F. Küppers, W. J. Heikkila, K. U. Kaila, and P. Tanskanen, Ground-based observations of an onset of localized field-aligned currents during auroral breakup and around local midnight, *J. Geophys.*, *48*, 101–115, 1980.

Pashin, A. B., K.-H. Glassmeier, W. Baumjohann, O. M. Raspopov, A. G. Yahnin, H. J. Opgenoorth, and R. J. Pellinen, Pi 2 magnetic pulsations, auroral break-up, and the substorm current wedge: A case study, *J. Geophys.*, *51*, 223–233, 1982.

Rees, M. H., Auroral ionization and excitation by incident energetic electrons, *Planet. Space Sci.*, *11*, 1209–1218, 1963.

Rostoker, G., and J. C. Samson, Polarization characteristics of Pi 2 pulsations and implications for their source mechanisms: Location of the source regions with respect to the auroral electrojets, *Planet. Space Sci.*, *29*, 225–247, 1981.

Rostoker, G., A. Vallance Jones, R. L. Gattinger, C. D. Anger, and J. S. Murphee, The development of the substorm expansive phase: The "eye" of the substorm, *Geophys. Res. Lett.*, *14*, 399–402, 1987.

Rothwell, P. L., M. B. Silevitch, and L. P. Block, A model for the propagation of the westward traveling surge, *J. Geophys. Res.*, *89*, 8941–8948, 1984.

Rothwell, P. L., M. B. Silevitch, and L. P. Block, Pi 2 pulsations and the westward traveling surge, *J. Geophys. Res.*, *91*, 6921–6928, 1986.

Rothwell, P. L., M. B. Silevitch, and L. P. Block, The motion of the WTS as a function of electron anisotropy in the plasma sheet, in *Modeling Magnetospheric Plasma, Geophys. Monogr. Ser.*, vol. 44, edited by T. E. Moore and J. H. Waite, AGU, Washington, D. C., in press, 1988.

Saito, T., Oscillation of the geomagnetic field with the progress of pt-type pulsation, *Sci. Rep. Tohoku Univ., Ser., 5*, *13*, 53, 1961.

Samson, J. C., Pi 2 pulsations: High latitude results, *Planet. Space Sci.*, *30*, 1239–1247, 1982.

Samson, J. C., and G. Rostoker, Polarization characteristics of Pi 2 pulsations and implications for their source mechanism: Influence of the westward travelling surge, *Planet. Space Sci.*, *31*, 435–458, 1983.

Sato, T., Auroral physics, in *Magnetospheric Plasma Physics*, edited by A. Nishida, pp. 197–243, D. Reidel, Hingham, Mass., 1982.

Silevitch, M. B., L. P. Block, C.-G. Fälthammar, G. Marklund, and M. A. Raadu, On the temporal evolution of enhanced conductivity regions associated with the westward traveling surge (abstract), *Eos Trans. AGU*, *65*, 1065, 1984.

Singer, H. J., D. J. Southwood, R. J. Walker, and M. G. Kivelson, Alfvén wave resonances in a realistic magnetospheric magnetic field geometry, *J. Geophys. Res.*, *86*, 4589–4596, 1981.

Singer, H. J., W. J. Hughes, P. J. Fougere, and D. J. Knecht, The localization of Pi 2 pulsations: Ground-satellite observations, *J. Geophys. Res.*, *88*, 7029–7036, 1983.

Singer, H. J., W. J. Hughes, C. Gelpi, and B. G. Ledley, Magnetic disturbances in the vicinity of the substorm current wedge: A case study, *J. Geophys. Res.*, *90*, 9583–9589, 1985.

Southwood, D. J., and W. F. Stuart, Pulsations at substorm onset, in *Dynamics of the Magnetosphere*, edited by S.-I. Akasofu, pp. 341–355, D. Reidel, Hingham, Mass., 1980.

Stuart, W. F., C. A. Green, and T. J. Harris, Correlation between modulation of the intensity of precipitating electrons in the auroral zone and a coincident Pi 2, *J. Atmos. Terr. Phys.*, *39*, 631–635, 1977.

Tanskanen, P., et al. Different phases of a magnetospheric substorm on June 23, 1979, *J. Geophys. Res.*, *92*, 7443–7457, 1987.

Weimer, D. R., C. K. Goertz, D. A. Gurnett, N. C. Maynard, and J. L. Burch, Auroral zone electric fields from DE 1 and 2 at magnetic conjunctions, *J. Geophys. Res.*, *90*, 7479–7494, 1985.

Weimer, D. R., D. A. Gurnett, C. K. Goertz, J. D. Menietti, J. L. Burch, and M. Sugiura, The current-voltage relationship in auroral current sheets, *J. Geophys. Res.*, *92*, 187–194, 1987.

Zhu, L., and J. R. Kan, Time evolution of the westward-traveling surge, *Planet. Space Sci.*, *35*, 145–151, 1987.

L. P. Block, Department of Plasma Physics, Royal Institute of Technology, S10044 Stockholm 70, Sweden.

P. L. Rothwell, Air Force Geophysics Laboratory, PHG, Hanscom AFB, Bedford, MA 01731.

M. B. Silevitch, Center for Electromagnetics Research, Northeastern University, Boston, MA 02115.

P. Tanskanen, Department of Physics, University of Oulu, SF-90570, Oulu, Finland.

(Received October 22, 1987;
revised January 22, 1988;
accepted February 25, 1988.)

Unclassified
SECURITY CLASSIFICATION OF THIS PAGE

REPORT DOCUMENTATION PAGE

1a REPORT SECURITY CLASSIFICATION Unclassified	1b RESTRICTIVE MARKINGS
2a SECURITY CLASSIFICATION AUTHORITY	3 DISTRIBUTION/AVAILABILITY OF REPORT
2b DECLASSIFICATION/DOWNGRADING SCHEDULE	
4 PERFORMING ORGANIZATION REPORT NUMBER(S) AFGL-TR-88-0185	5 MONITORING ORGANIZATION REPORT NUMBER(S)
6a NAME OF PERFORMING ORGANIZATION Air Force Geophysics Laboratory 6b OFFICE SYMBOL (If applicable) PHG	7a NAME OF MONITORING ORGANIZATION
6c ADDRESS (City, State, and ZIP Code) Hanscom AFB Massachusetts, 01731-5000	7b ADDRESS (City, State, and ZIP Code)
8a NAME OF FUNDING/SPONSORING ORGANIZATION 8b OFFICE SYMBOL (If applicable)	9 PROCUREMENT INSTRUMENT IDENTIFICATION NUMBER
8c ADDRESS (City, State, and ZIP Code)	10 SOURCE OF FUNDING NUMBERS PROGRAM ELEMENT NO: 61102F; PROJECT NO: 2311; TASK NO: G5; WORK UNIT ACCESSION NO: 01

11 TITLE (Include Security Classification)
A Model of the Westward Traveling Surge and the Generation of Pi 2 Pulsations

12 PERSONAL AUTHOR(S)
P.L. Rothwell, M.B. Silevitch*, L.P. Block**, P. Tanskanen#

13a TYPE OF REPORT	13b TIME COVERED	14 DATE OF REPORT (Year, Month, Day)	15 PAGE COUNT
Reprint	FROM ____ TO ____	1988 Sep 7	12

16 SUPPLEMENTARY NOTATION *Center for Electromagnetics Research, Northeastern University, Boston, Massachusetts, **Department of Plasma Physics, Royal Institute of Technology, Stockholm Sweden, #Department of Physics, University of Oulu, Oulu, Finland - Reprinted from Journal of Geophysical Research, Vol. 93, No. A8, pages 8613-8624, August 1, 1988

17 COSATI CODES		
FIELD	GROUP	SUB-GROUP

18 SUBJECT TERMS (Continue on reverse if necessary and identify by block number)
Westward Traveling Surge, Ionosphere, Aurora

19 ABSTRACT (Continue on reverse if necessary and identify by block number)

A model of the westward traveling surge (WTS) and the generation of Pi 2 pulsations is presented here. Previous work concentrated on the motion of the WTS as a function of the precipitating electron energy and the collisionless generation of Pi 2 pulsations via a feedback instability. Now we look in more detail at the physical assumptions used in deriving the present model and the relations between the zero-order and the first-order solutions. Constraints are placed on the electron temperature asymmetry in the plasma sheet by requiring the Pi 2 pulsations to be bounded. It is found that the electron temperature anisotropy in the plasma sheet plays a major role in determining the direction in which the surge will first propagate. Narrower surges require greater electron heating parallel to the magnetic field for poleward motion. More energetic electron precipitation is predicted to produce higher-frequency Pi 2 pulsations. Pulsations occur in multiple bursts with the time interval between bursts being shorter for shorter field lines. Initial amplitude and phase conditions are crucial in determining the pulse shape. The dominant period of the Pi 2 pulsation is found to be equal to twice the north-south dimension of the surge divided by a term which is proportional to the poleward velocity of the boundary. Finally, we show that the poleward surge velocities and Pi 2 pulsation periods as measured during the magnetospheric substorm of June 23, 1979, are consistent with our model. By noting the direction of the surge motion, one can use the model to estimate the magnitude of the polarization electric field. We find that it is consistent with values for the onsets as modeled.

20 DISTRIBUTION/AVAILABILITY OF ABSTRACT	21 ABSTRACT SECURITY CLASSIFICATION
☐ UNCLASSIFIED/UNLIMITED ☐ SAME AS RPT ☐ DTIC USERS	Unclassified
22a NAME OF RESPONSIBLE INDIVIDUAL P.L. Rothwell	22b TELEPHONE (Include Area Code) (617) 377-2431 22c OFFICE SYMBOL PHG

DD FORM 1473, 84 MAR 83 APR edition may be used until exhausted
All other editions are obsolete.

SECURITY CLASSIFICATION OF THIS PAGE
Unclassified

88 9 12 114